

AN ENERGETIC AFTERGLOW FROM A DISTANT STELLAR EXPLOSION

D. A. FRAIL¹, P. B. CAMERON², M. KASLIWAL², E. NAKAR⁴, P. A. PRICE³, E. BERGER^{5,6,7},
 A. GAL-YAM^{2,7}, S. R. KULKARNI², D. B. FOX⁸, A. M. SODERBERG², B. P. SCHMIDT⁷, E. OFEK²,
 AND S. B. CENKO⁹

Draft version May 8, 2018

ABSTRACT

We present the discovery of radio afterglow emission from the high redshift ($z = 6.295$) burst GRB 050904. The peak flux density for this burst is similar to typical low-redshift gamma-ray bursts (GRB). We further show that beyond a redshift of order unity, the flux density of radio afterglows are largely insensitive to redshift, consistent with predictions. By combining the existing X-ray, near-infrared and radio measurements, we derive estimates for the kinetic energy and opening angle of the blast wave, and for the density of the circumburst medium into which it expands. Both the kinetic and radiated energy indicate that GRB 050904 was an unusually energetic burst (10^{52} erg). More importantly, we are able to make an *in situ* measurement of the density structure of the circumburst medium. We conclude that GRB 050904 exploded into a constant density medium with $n_0 = 680 \text{ cm}^{-3}$, which is two orders of magnitude above the nominal value for low-redshift GRBs. The next generation of centimeter (EVLA) and millimeter radio instruments (ALMA) will be able to routinely detect events like GRB 050904 and use them to study magnetic fields, and the atomic and molecular gas in the high redshift Universe.

Subject headings: gamma-ray bursts: specific (GRB 050904)

1. INTRODUCTION

Understanding the reionization of the Universe, when the first luminous sources were formed, is one of the latest frontiers of observational cosmology. Constraints have been obtained using diagnostics such as quasar studies of the Gunn-Peterson absorption trough, the luminosity evolution of Ly α galaxies, and the polarization isotropy of the cosmic microwave background. Taken together, these data portray a complicated picture in which reionization has taken place over a wide range of redshifts ($6 \leq z \leq 20$) rather than at one specific epoch. The dominant source of reionization appears to be due to ultraviolet emission from young, massive stars (see review by Fan, Carilli & Keating 2006).

As the most luminous explosions in the Universe, gamma-ray bursts (GRBs) are potential signposts of these early massive stars. The radio, infrared and X-ray afterglow emission from GRBs are in principle observable out to $z \sim 30$ (Miralda-Escude 1998; Lamb & Reichart 2000; Ciardi & Loeb 2000; Gou *et al.* 2004; Ioka & Mészáros 2005). It is estimated that 10% of GRBs detected by the *Swift* satellite are at $z > 5$ (Natarajan *et al.* 2005; Bromm & Loeb 2006). The most distant GRB to date is GRB 050904 at $z = 6.295$. It was detected by the *Swift*

Burst Alert Telescope and localized to an accuracy of a few arcseconds by the *Swift* X-ray Telescope (Gehrels *et al.* 2004). Follow-up optical and near-infrared observations (NIR) were begun shortly thereafter. Details on the discovery and properties of the X-ray and NIR afterglow of this burst can be found in several papers (Cusumano *et al.* 2006; Haislip *et al.* 2006; Boer *et al.* 2006). An optical/NIR spectrum taken by the *Subaru* telescope 3.4 days after the burst showed multiple heavy metal absorption lines and a Gunn-Peterson trough with a damping wing redward of the Ly α cutoff which was used to derive the neutral fraction $x_H < 0.6$ (Totani *et al.* 2005; Kawai *et al.* 2006). With a *Swift* GRB detection rate of 100 yr^{-1} , GRBs could one day replace quasars as the preferred probe of the high redshift Universe.

In this paper we report on the detection of the radio afterglow from GRB 050904 (§2), which makes it possible to derive physical properties of the explosion and the circumburst medium (§3). Our results are compared with predictions for the properties of the explosion and how the progenitors of high redshift GRBs are expected to have shaped their surrounding environments (§4).

2. OBSERVATIONS AND RESULTS

¹National Radio Astronomy Observatory, Socorro, NM 87801

²Division of Physics, Mathematics and Astronomy, 105-24, California Institute of Technology, Pasadena, CA 91125

⁴Theoretical Astrophysics, California Institute of Technology, MS 130-33, Pasadena, CA 91125

⁵Observatories of the Carnegie Institution of Washington, 813 Santa Barbara Street, Pasadena, CA 91101

⁶Princeton University Observatory, Peyton Hall, Ivy Lane, Princeton, NJ 08544

⁷Hubble Fellow

³Institute for Astronomy, University of Hawaii, 2680 Woodlawn Drive, Honolulu, HI 96822

⁸Research School of Astronomy and Astrophysics, Australian National University, Mt Stromlo Observatory, via Cotter Rd, Weston Creek, ACT 2611, Australia

⁹Department of Astronomy and Astrophysics, Pennsylvania State University, 525 Davey Laboratory, University Park, PA 16802

¹⁰Space Radiation Laboratory, MS 220-47, California Institute of Technology, Pasadena, CA 91125

¹⁰Gemini Observatory, 670 N. Aohoku Place Hilo, HI 96720

Radio observations were undertaken with the Very Large Array¹² (VLA) at a frequency of 8.46 GHz (see Table 1). To maximize sensitivity, the full VLA continuum bandwidth (100 MHz) was recorded in two 50 MHz bands. Data reduction was carried out following standard practice in the *AIPS* software package. Some additional phase and amplitude self-calibration was necessary to remove the contaminating effects of a bright (10 mJy) radio source four arcminutes northeast from the GRB.

Radio emission from GRB 050904 was not detected during the first week, ruling out a bright short-lived component similar to GRB 990123 (Kulkarni *et al.* 1999). By averaging the data from this period, we obtain a peak flux at the position of the NIR afterglow of 33 ± 14 uJy. A clear detection was made during three epochs 34–37 days after the burst (see Table 1). Averaging the data taken in October we obtain a mean flux density of 76 ± 14 uJy. The spectral radio luminosity, expressed as $L_\nu = 4\pi F_\nu d_L^2 (1+z)^{\alpha-\beta-1} = 2.5 \times 10^{31} \text{ erg s}^{-1} \text{ Hz}^{-1}$ (where $F_\nu \propto t^\alpha \nu^\beta$ and $\alpha \sim 0$ and $\beta = 1/3$ has been assumed, corresponding to an optically thin, flat post-jet break light curve), is normal for GRBs (Soderberg *et al.* 2004), and is two orders of magnitude below the highest redshift radio-loud quasars (Carilli *et al.* 2004).

We show these detections in Fig. 1 together with a complete sample of 8.5 GHz flux density measurements for GRBs with known redshifts. Neither the time-to-peak nor the flux density of GRB 050904 is unusual compared to the known sample of GRBs at lower redshifts. In the source rest frame the flux density for the majority of afterglows is reached before 5 days postburst. More interestingly, the average centimeter flux density in Fig. 1 shows only a weak dependence on redshift.

This effect was predicted by Ciardi & Loeb (2000) and is shown here for the first time. It is reminiscent of the “negative k-correction” for submillimeter observations of ultraluminous infrared galaxies (Blain *et al.* 2002). The afterglow flux density remains high because of the dual effects of spectral and temporal redshift, offsetting the dimming due to the increase in distance (Lamb & Reichart 2000). We illustrate in Fig. 1 how slowly the centimeter flux density decreases for a canonical GRB afterglow beyond $z \sim 1$ due to this effect (long dashed lines), compared to one whose luminosity is assumed constant (short dashed lines). Observational bias does not explain the flattening in Fig. 1 because the detection rate of radio afterglows is largely insensitive to redshift. Of the 60 GRBs with known redshift that have been observed in the radio, there are 42 with detected afterglows. Their detection rate above and below $z = 1$ is identical.

3. AFTERGLOW MODELING

We now proceed to combine these radio data (§2) with the extensive X-ray and optical/NIR data for GRB 050904 in order to constrain the physical parameters of the outflow and the circumburst medium. We interpret these multi-wavelength data within the framework of the relativistic blastwave model (see Mészáros 2002 for a review). The particular fitting approach that we take is described in more detail in Yost *et al.* (2003).

To limit the number of free parameters in the fit, we chose to model only the evolution of the forward shock after energy injection has ceased. The early X-ray light curve shows complex flaring activity, common in *Swift* bursts but lasting an unusually long time ($\Delta t < 0.7$ days), corresponding to a central engine lifetime of more than 2 hrs in the source rest frame (Cusumano *et al.* 2006). On-going energy injection is also suspected based on the flares and the flattening of the optical/NIR lightcurves on similar timescales (Boer *et al.* 2006; Haislip *et al.* 2006). If these early data are excluded the NIR data show a smooth power-law evolution with a clear break at $t_j = 2.6 \pm 1.0$ days and decay indices before and after the break of $\alpha_1 = -0.72^{+0.15}_{-0.20}$ and $\alpha_2 = -2.4 \pm 0.4$ (Tagliaferri *et al.* 2005). If interpreted as a jet break, the sharpness of the transition makes it unlikely that this burst occurred in a wind-blown environment (Kumar & Panaitescu 2000) and motivates our modeling choice of a constant density circumburst medium.

Our best-fit forward shock model is shown in Fig. 2. We fit for the isotropic kinetic energy of the shock $E_{k,iso,52}$, the opening angle of the jet θ_j , the density of the circumburst medium n_o , the electron energy index p , and the fraction of the shock energy density in relativistic electrons ϵ_e and magnetic fields ϵ_B .

Our model makes the unusual prediction that the synchrotron cooling frequency lies below *both* the X-ray and optical bands before the first J-band detection of the afterglow at $\Delta t = 3.07$ hrs (Haislip *et al.* 2006). This implies a steep spectral slope of $\beta = -p/2 = -1.07$ (Sari, Piran & Halpern 1999). This is likely the case at $\Delta t = 3$ days where we derive an NIR/X-ray slope of $\beta_{ox} = -1.1 \pm 0.05$. This value also agrees with Tagliaferri *et al.* (2005) who derive a best fit optical/NIR spectral index of $\beta_o = -1.25 \pm 0.25$ over the interval from 0.4 to 7 days postburst. A steep spectral slope of $\beta_x \sim -0.85$ is seen even when the X-ray light curve is highly time variable between $0.05 \leq \Delta t \leq 0.7$ days. Thus we find that the available data support a small value for the cooling frequency.

Our best-fit model favors a circumburst density $n_o = 680 \text{ cm}^{-3}$. To test the robustness of this result we ran several model fits, fixing n_o over a range of values between 0.7 cm^{-3} and $7 \times 10^4 \text{ cm}^{-3}$. As expected, the X-ray and NIR data are relatively insensitive to n_o , so the radio afterglow provides the tightest constraints. Large densities $n_o > 10^4 \text{ cm}^{-3}$ are ruled out since the solutions are bounded by the condition that the magnetic and electron densities do not exceed equipartition. Low densities $n_o < 10 \text{ cm}^{-3}$ are also not favored since they predict bright early radio emission in the first week well in excess of that which is observed (§2). Over the allowable density range, $E_{k,iso,52}$ varies from 40 to 530, and therefore it is no better constrained by the afterglow data than the *isotropic* radiated energy $E_{\gamma,iso,52}$ is by the prompt emission (Cusumano *et al.* 2006).

Another possibility is that radio afterglow flux density measurements are biased by the turbulent ionized interstellar medium of our Galaxy which induces non-Gaussian intensity fluctuations for compact radio sources. Indeed, it has been shown by Cordes & Lazio (1991) that repeated

¹²The Very Large Array is operated by the National Radio Astronomy Observatory, a facility of the National Science Foundation operated under cooperative agreement by Associated Universities, Inc.

short observations similar to those in Table 1 increase the odds of detecting a weak radio signal close to the detection threshold. We replaced the detections with upper limits and re-ran the fit. High density solutions are still preferred ($n_o \simeq 10^4 \text{ cm}^{-3}$) because both the X-ray and optical afterglows of GRB 050904 were bright (Cusumano *et al.* 2006; Haislip *et al.* 2006). Thus, in order to suppress the radio emission at 8.5 GHz (or 62 GHz in the rest frame), a large value of the synchrotron self-absorption is required and hence a large circumburst density.

4. DISCUSSION

With the detection of the radio afterglow from GRB 050904 we have a complete multi-wavelength dataset for this high redshift burst. By comparing the physical properties of the burst and its circumburst environment to those GRBs found at lower redshifts, we hope to gain some insight into the birth and death of the earliest generations of stars in the Universe.

There is good support for interpreting GRB 050904 as an energetic event. From our afterglow modeling (§3) of the isotropic kinetic energy of the shock $E_{k,iso,52} = 88$ (normalized in units of 10^{52} erg). Estimates obtained for the *isotropic* radiated energy (Cusumano *et al.* 2006) with $66 \leq E_{\gamma,iso,52} \leq 320$. The quoted range in $E_{\gamma,iso,52}$ reflects the uncertainty in the location of the peak of the gamma-ray spectrum. These constraints can be refined owing to our fitting the jet opening angle $\theta_j=0.14$ rad (see also Tagliaferri *et al.* 2005). The geometrically corrected energies are $E_{k,52} \simeq E_{k,iso,52} \times \theta_j^2/2=0.9$, and $0.7 \leq E_{\gamma,52} \leq 3$. Both the radiated and kinetic energy of this event lie at or beyond the values derived for a large sample of lower redshift afterglows (Panaiteanu & Kumar 2001, 2002; Yost *et al.* 2003; Friedman & Bloom 2005). An independent check on this result uses the X-ray light curve to compute the geometrically-corrected X-ray luminosity at some fiducial time (usually taken at $\Delta t=10$ hrs). We derive $L_x=2.6 \times 10^{45} \text{ erg s}^{-1}$, again larger than any previous GRB afterglow (Berger, Kulkarni & Frail 2003).

Perhaps the most interesting aspect of these data is that they allow us to make an *in situ* measurement of the density structure for a massive star in the early Universe. From our afterglow modeling we conclude that

GRB 050904 exploded into a constant density medium with $n_o=680 \text{ cm}^{-3}$ – two orders of magnitude above the nominal value for lower redshift GRBs (Friedman & Bloom 2005; Soderberg *et al.* 2006). Line-of-sight measures (Cusumano *et al.* 2006; Haislip *et al.* 2006; Totani *et al.* 2005) also indicate that a substantial column of gas exists towards GRB 050904. The fine-structure silicon lines SiII* are the most important since their column density ratios yield estimates of the electron density $n_e \sim 10^{2.3 \pm 0.7} \text{ cm}^{-3}$ (Kawai *et al.* 2006). The close agreement of this line-of-sight estimate with our *in situ* value argues for a common physical origin for the gas in the immediate vicinity of the GRB.

There are testable predictions for star formation and collapse in the early Universe (Bromm & Loeb 2006 and reference therein). The first stars are expected to be very massive and could produce energetic GRB explosions like GRB 050904. Likewise, the high density we derived for GRB 050904 may be part of the general increase expected for the ambient density of the interstellar medium (Ciardi & Loeb 2000), but more likely just indicates that this GRB exploded in a dense molecular cloud. A lower density would be expected if the progenitor of GRB 050904 was a low metallicity Wolf-Rayet star (Vink & de Koter 2005). However, it remains a problem, at both low and high redshifts, why the radial density signature from the collapsar wind is rarely detected (Chevalier, Li & Fransson 2004). A larger sample is needed before drawing too much from these predictions. Deep radio observations will continue to play a role since can be seen out to the highest redshifts and are sensitive probes of the total calorimetry of the explosion and the density structure of the circumburst medium. Looking further ahead to the next generation of centimeter (EVLA) and millimeter radio instruments (ALMA), events like GRB 050904 will be bright enough to sample primordial magnetic fields (Gaensler, Beck & Feretti 2004), and probe the cold atomic and molecular gas from the time of the first light (Inoue, Omukai & Ciardi 2005).

DAF wishes to thank B. Clark for his generous allocation of VLA time during the dynamic scheduling tests.

References

- Berger, E., Kulkarni, S. R., and Frail, D. A. 2003, ApJ, 590, 379.
- Bessell, M. S., Castelli, F., and Plez, B. 1998, A&A, 333, 231.
- Blain, A. W., Smail, I., Ivison, R. J., Kneib, J.-P., and Frayer, D. T. 2002, Physics Reports, 369, 111.
- Boer, M. *et al.* 2006, astro-ph/0510381.
- Bromm, V. and Loeb, A. 2006, ApJ, in press.
- Carilli, C. L. *et al.* 2004, AJ, 128, 997.
- Chevalier, R. A., Li, Z., and Fransson, C. 2004, ApJ, 606, 369.
- Ciardi, B. and Loeb, A. 2000, ApJ, 540, 687.
- Cordes, J. M. and Lazio, T. J. 1991, ApJ, 376, 123.
- Cusumano, G. *et al.* 2006, Nature in press; astro-ph/0509737.
- Fan, X., Carilli, C. L., and Keating, B. 2006, An. Rev. Astron. & Astro.; astro-ph/0602375.

- Frail, D. A., Kulkarni, S. R., Berger, E., and Wieringa, M. H. 2003, *AJ*, 125, 2299.
- Friedman, A. S. and Bloom, J. S. 2005, *ApJ*, 627, 1.
- Gaensler, B. M., Beck, R., and Feretti, L. 2004, *New Astronomy Review*, 48, 1003.
- Gehrels, N. *et al.* 2004, *ApJ*, 611, 1005.
- Gou, L. J., Mészáros, P., Abel, T., and Zhang, B. 2004, *ApJ*, 604, 508.
- Haislip, J. *et al.* 2006, submitted to *Nature*; astro-ph/0509660.
- Inoue, S., Omukai, K., and Ciardi, B. 2005, *MNRAS*; astro-ph/0502218.
- Ioka, K. and Mészáros, P. 2005, *ApJ*, 619, 684.
- Kawai, N. *et al.* 2006, *Nature* submitted; astro-ph/0512052.
- Kulkarni, S. R. *et al.* 1999, *ApJ*, 522, L97.
- Kumar, P. and Panaitescu, A. 2000, *ApJ*, 541, L9.
- Lamb, D. Q. and Reichart, D. E. 2000, *ApJ*, 536, 1.
- Mészáros, P. 2002, *Ann. Rev. Astr. Ap.*, 40, 137.
- Miralda-Escude, J. 1998, *ApJ*, 501, 15.
- Natarajan, P., Albanna, B., Hjorth, J., Ramirez-Ruiz, E., Tanvir, N., and Wijers, R. 2005, *MNRAS*, 364, L8.
- Panaitescu, A. and Kumar, P. 2001, *ApJ*, 554, 667.
- Panaitescu, A. and Kumar, P. 2002, *ApJ*, 571, 779.
- Sari, R., Piran, T., and Halpern, J. P. 1999, *ApJ*, 519, L17.
- Schlegel, D. J., Finkbeiner, D. P., and Davis, M. 1998, *ApJ*, 500, 525.
- Soderberg, A. M. *et al.* 2004, *ApJ*, 606, 994.
- Soderberg, A. M., Nakar, E., Berger, E., and Kulkarni, S. R. 2006, *ApJ*, 638, 930.
- Tagliaferri, G. *et al.* 2005, *A&A*, 443, L1.
- Totani, T. *et al.* 2005, Submitted to *PASJ*; astro-ph/0512154.
- Vink, J. S. and de Koter, A. 2005, *A&A*, 442, 587.
- Yost, S. A., Harrison, F. A., Sari, R., and Frail, D. A. 2003, *ApJ*, 597, 459.

TABLE 1
RADIO OBSERVATIONS

Date Obs (UT)	Δt (days)	F_ν^a (μJy)
2005 Sep. 4.58	0.50	89 ± 58
2005 Sep. 5.48	1.40	41 ± 25
2005 Sep. 9.48	5.40	-3 ± 25
2005 Sept. 10.31	6.23	27 ± 24
2005 Sep. 24.20	20.12	89 ± 37
2005 Oct. 3.36	29.28	40 ± 30
2005 Oct. 7.30	33.22	-10 ± 35
2005 Oct. 8.26	34.18	64 ± 23
2005 Oct. 9.34	35.26	116 ± 18
2005 Oct. 11.43	37.35	67 ± 17
2005 Oct. 18.37	44.29	13 ± 27

^aAll errors are given as 1σ (rms).

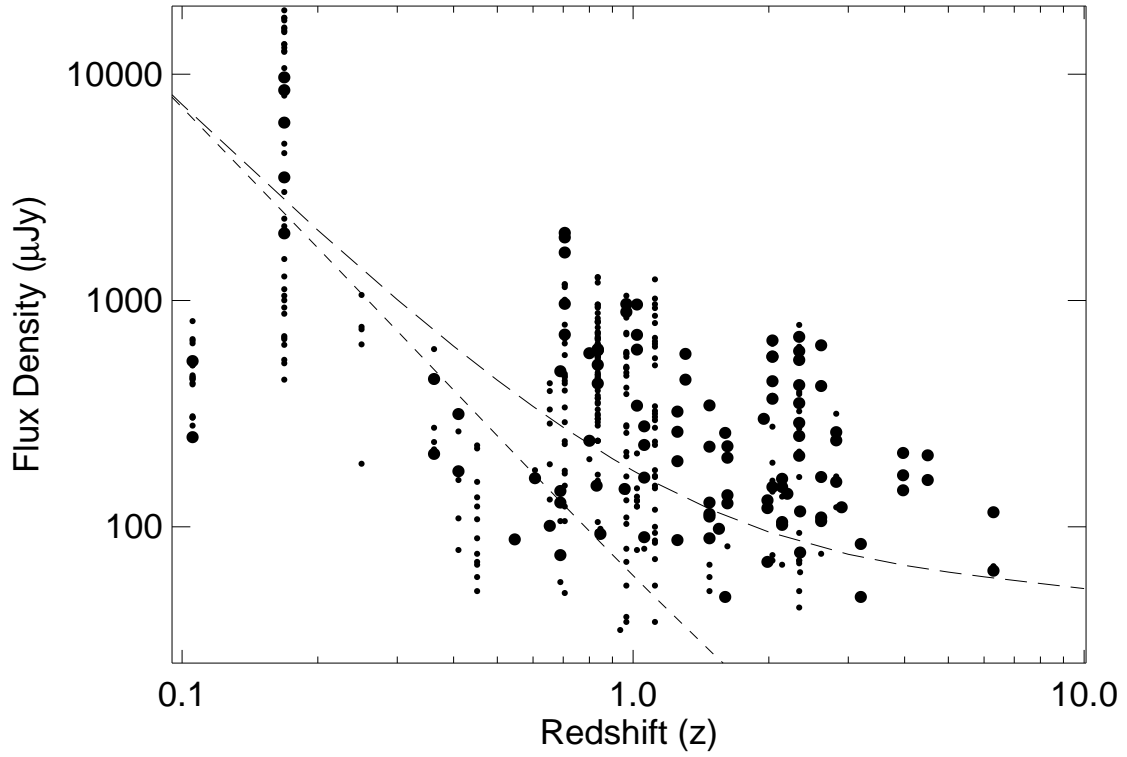


FIG. 1.— Radio flux density versus redshift for a complete sample of 60 bursts observed at radio wavelengths from 1997 to 2006. The radio measurements were made at 8.5 GHz and are taken from Frail *et al.* (2003) and the public radio afterglow database (http://www.aoc.nrao.edu/~dfrail/grb_public.shtml). For clarity only the 42 GRBs with known redshifts and radio afterglow detections are plotted. The large (small) circles indicate measurements taken less (more) than 5 days before (after) the burst in its rest frame. The long dashed line is the flux density for a canonical afterglow model at $\Delta t=5$ days (in the observer frame). It assumes $E_{k,iso,52} = 10^{53}$ erg, $\theta_j = 0.1$ rad, $n_o = 10 \text{ cm}^{-3}$, $p = 2.2$, $\epsilon_e=0.1$, and $\epsilon_B=1\%$ (see text for more details). The short dashed line shows the expected decrease if the flux scales simply as the inverse square of the luminosity distance.

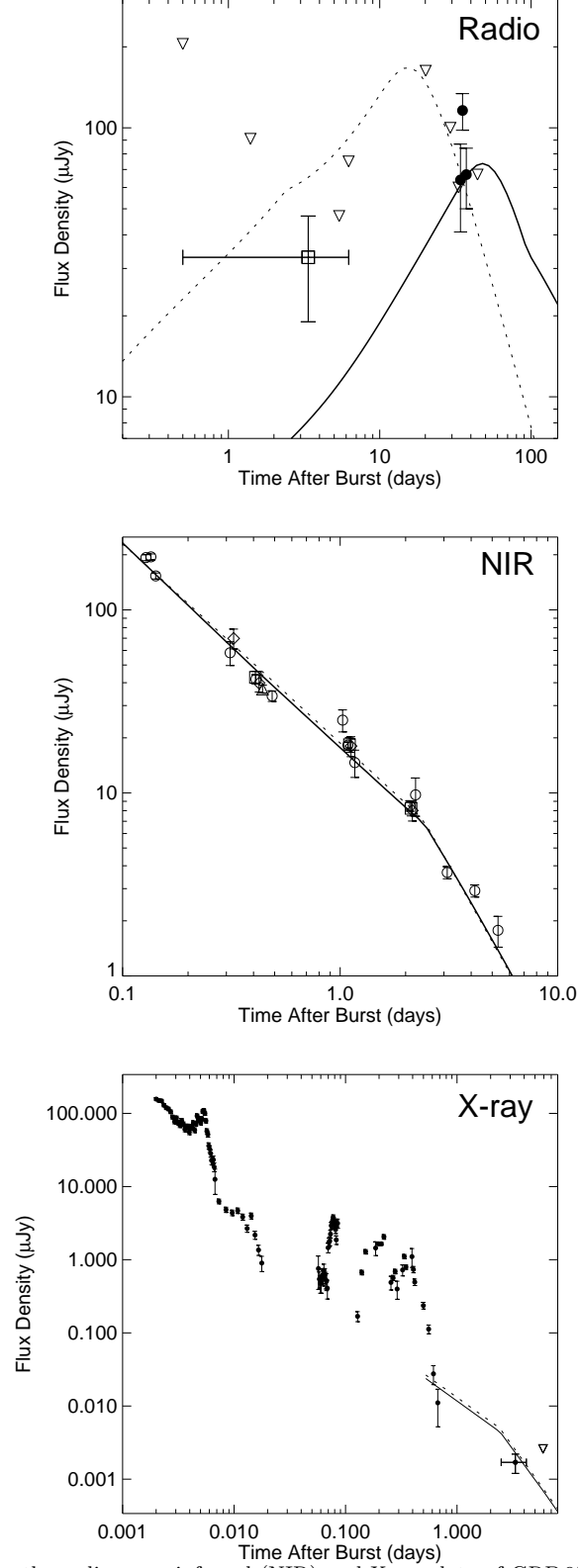


FIG. 2.— Broad-band afterglow fits for the radio, near infrared (NIR) and X-ray data of GRB 050904. The radio data are taken from §2. Solid circles indicate detections, upper limits are inverted triangles (plotted as flux + 2σ). The open square is the peak flux obtained by averaging the first week of data. The NIR data are taken from Tagliaferri *et al.* (2005) and Haislip *et al.* (2006), with a small correction made for Galactic dust extinction (Schlegel, Finkbeiner & Davis 1998) before converting to flux density (Bessell, Castelli & Plez 1998). JHK and K' are shown for display purposes on the same plot after scaling by the best-fit spectral index. We have converted the *Swift* X-ray data (0.2–10 keV) to flux density using the average photon index $\Gamma = -1.84$ and a frequency of 2.8×10^{17} Hz (see Cusumano *et al.* 2006). The solid line is our best-fit forward shock model for a constant density circumburst medium with $E_{k,iso,52} = 8.8 \times 10^{53}$ erg, $\theta_j = 0.14$ rad, $n_o = 680$ cm $^{-3}$, $p = 2.14$, $\epsilon_e = 2.0\%$, and $\epsilon_B = 1.5\%$ (see text for more details). The thin dashed line shows the effect of model fitting when the value of n_o is fixed at 100 times lower than the best-fit value.